

Grating polychromator with a multichannel photodetector

T.M. Petrova and L.N. Sinita

*Institute of Atmospheric Optics,
Siberian Branch of the Russian Academy of Sciences, Tomsk*

Received August 11, 2003

A grating spectrometer with a CCD photorecording system operating in the near infrared and visible spectral regions is presented. The spectrometer has the spectral resolution of 0.036 cm^{-1} and allows recording of absorption spectra with the accuracy of 0.003 cm^{-1} in line positions and 3% in the absorption coefficient. Absorption spectra of the atmospheric air were recorded with a 1-m long absorbing layer.

Introduction

Recent years in experimental spectroscopy are characterized by successful development of Fourier transform and laser spectroscopy instrumentation. Such devices have high spectral resolution and sensitivity and, while at the same time, by high costs. In contrast, devices of classical spectroscopy, in particular, grating spectrometers are paid only little attention. At the same time, the development of recording instrumentation – multichannel photodetectors (CCD and photodiode arrays) opens new possibilities in fabrication of grating polychromators allowing recording of 2000 and more spectral elements, simultaneously.

In this paper we consider a grating spectrometer based on a linear CCD array intended for investigation of molecular spectra in the visible spectral region.

1. The instrumentation

The basic element of the spectrometer is a DFS-8 high-resolution spectrograph designed by the Ebert vertically symmetric autocollimation optical arrangement with the objective's focal length of 2650 mm. The spectrograph includes a diffraction grating with 1800 grooves/mm, which is operated in the first diffraction order at the diffraction angles of $35\text{--}75^\circ$. The photodetector was assembled based on a Sony 1LX511 linear CCD array having 2048 elements and the length of $\sim 28 \text{ mm}$. More detailed description of its operation can be found in Ref. 1.

The block-diagram of the experimental setup is shown in Fig. 1. As a radiation source, it employs a 50-W cw halogen lamp. An objective with 8-cm focal length is used to form a parallel beam, which passes through an 1-m long cell with the analyzed substance. It was possible to heat the cell up to 1100 K. The lamp radiation was focused onto the entrance slit. To increase the radiation intensity, we used an extra spherical reflector, whose focus coincided with the radiation source.

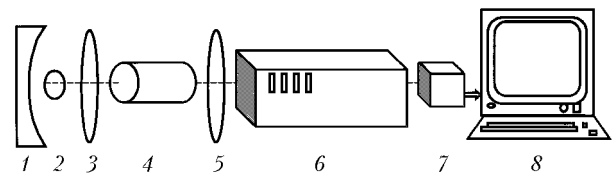


Fig. 1. Grating polychromator: spherical reflector 1, radiation source 2, lenses 3 and 5, cell with the analyzed substance 4, grating spectrograph 6, CCD photodetector 7, computer 8.

2. Parameters of the spectrometer

1. *The spectral range isolated* is determined by the sensitive region of the photodetector, which is 400–1000 nm for Sony 1LX511 linear CCD array, and in the longwave region the sensitivity decreases drastically.

2. *The inverse linear dispersion* varies within the spectral range from 0.11 to 0.12 nm/mm. The 1800 grooves/mm diffraction grating in the region of 940 nm operates at the diffraction angles of $\sim 56^\circ$ and provides for the inverse linear dispersion $D_1 = 0.11 \text{ nm/mm}$.

3. *The normal slit width* is the width of the entrance slit, at which its geometric image in the focal plane is equal to the separation from the maximum to the first minimum at diffraction at the aperture of the wave incident on the diffraction grating:

$$S_n = \lambda f_1 / D \quad (1)$$

where f_1 is the focal length; λ is the wavelength; D is the input aperture diameter.²

For the wavelength of $0.9 \mu\text{m}$ at the focal length $f_1 = 2650 \text{ mm}$, the calculated normal slit width at the beam diameter $D = 90 \text{ mm}$ is $S_n = 0.026 \text{ mm}$. Figure 2 shows the width of the emission line of neon in a laser gas-discharge tube as a function of the entrance slit width S_1 .

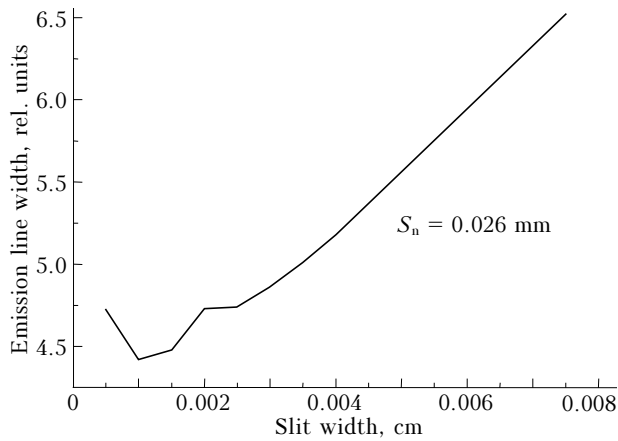


Fig. 2. The line width of the Ne emission in laser tube vs. the entrance slit width.

It can be seen that at S_1 smaller than 0.026 mm the dependence is no longer linear and diffraction at the beam aperture begins to manifest itself, which corresponds to the calculated value of S_n .

4. Instrumental function of the spectrometer.

The instrumental function of a spectral device distorts the spectra recorded. The relation between the true profile of a spectral line $F(\nu)$ and the directly measured profile $I(\nu')$ is described by the convolution equation

$$I(\nu') = \int_{-\infty}^{\infty} F(\nu) A(\nu' - \nu) d\nu, \quad (2)$$

where $A(\nu' - \nu)$ is the instrumental function.³ Thus, determination of the true profile of a spectral line from the measured one and the known instrumental function is reduced to solution of the integral equation, whose kernel is the true profile $F(\nu)$ sought. Having known $I(\nu')$ and $A(\nu' - \nu)$, we can find $F(\nu)$ – the true profile of a spectral line. The rigorous consideration of all the factors forming the instrumental function is usually impossible, practically measured $I(\nu')$ and $A(\nu' - \nu)$ often have too a complicated form, and it is rather difficult to solve Eq. (2).

Therefore, the instrumental function is usually determined experimentally through approximation by known functions. The instrumental function for different spectral devices may have the diffraction, Lorentz, Gauss, Voigt, and other profiles. For analysis of the instrumental function, light sources, whose line profile is known and narrow enough, for example, laser or atomic lines, are used. In this work, we used the lines of neon emission in the laser gas-discharge tube.

Since the gas pressure in the discharge tube was low (1–10 mm Hg), neon spectral lines had the Doppler profile, whose halfwidth can be estimated as follows:

$$\gamma_{\text{Ne}} = 3.58 \cdot 10^{-7} \sqrt{\frac{T}{\mu}} \frac{1}{\lambda}, \quad (3)$$

where λ is the central wavelength of a line; T is the gas temperature; μ is the atomic weight of emitting particles. Having known the gas temperature in the

laser tube ($T \sim 400$ K, see Ref. 4), $\mu = 20$, $\lambda = 950$ nm, we can estimate the neon line halfwidth in the near-IR region as $\gamma_{\text{Ne}} = 0.016 \text{ cm}^{-1}$.

We have recorded the neon line with the wavelength $\lambda = 945.921$ nm at $S_1 = S_n$. The profile consisted of 12 to 14 points. The results of fitting are shown in Fig. 3.

For approximation we used different spectral line profiles: Gauss, Lorentz, and Voigt ones. For the Lorentz profile we observed a considerable discrepancy between the experimental and calculated data, for the Gauss and Voigt profile the agreement was closer, but the halfwidth γ_L for the Voigt profile turned out to be ill-defined.

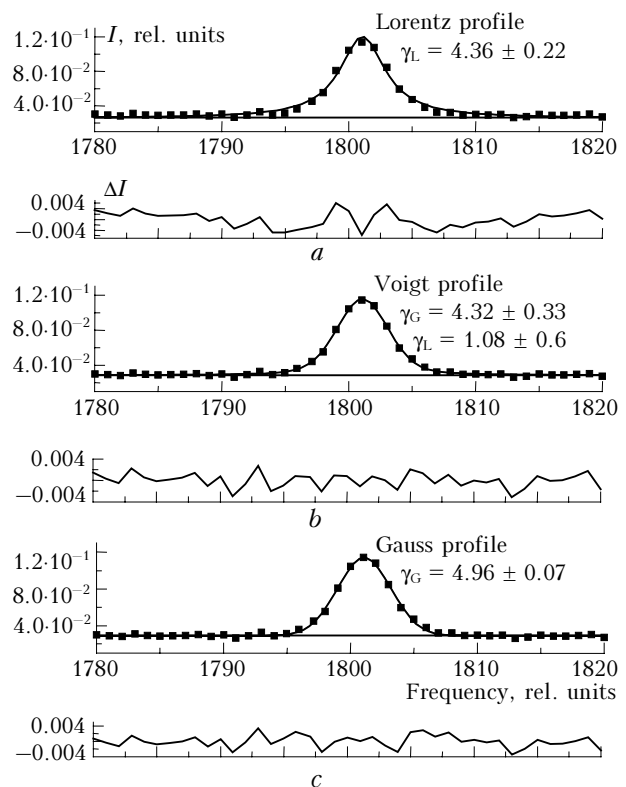


Fig. 3. Determination of instrumental function halfwidth. Approximation of the Ne emission line by the Lorentz (a), Voigt (b), and Gauss (c) profiles.

This analysis shows that the best result is obtained if using the Gauss profile γ_G , whose halfwidth is $\gamma = 0.040 \pm 0.005 \text{ cm}^{-1}$. Using Eq. (2) and the corresponding distributions, we can show that $\gamma_G^2 = \gamma_{\text{Ne}}^2 + \gamma_{\text{instr}}^2$. And, consequently, the halfwidth of the instrumental function is $\gamma_{\text{instr}} = 0.036 \text{ cm}^{-1}$.

5. The spectral resolution of the spectrometer developed is restricted by two factors. The first one is the spectral resolution provided by the diffraction grating. It is determined as

$$R = kn,$$

where n is the total number of grooves of the diffraction grating, which is equal to 2160000 in our case, and $k = 1$ is the diffraction order of the grating

used. Another factor restricting the spectral resolution is the spectral interval between two elements of the linear CCD array, equal to 0.016 cm^{-1} in the region of 900 nm . This factor contributes more significantly and determines the spectral resolution of 0.036 cm^{-1} , which agrees well with the width of the instrumental function.

6. *Determination of the line position.* The spectral interval between two elements of the CCD array in this particular instrument is 0.016 cm^{-1} , which provides for a sufficiently large number of points on the lines under study (10–12 points within the width of a Doppler profile of an H_2O line and 20–22 points within the air pressure broadened H_2O line width).

To calibrate the frequency scale of the spectrometer, we used reference lines. The frequencies of the measured lines were interpolated with respect to the frequencies of the reference lines known with high accuracy. The reference spectrum should include large enough number of lines. The neon spectrum in discharge meets these requirements quite well.⁵ In the visible range, several lines were observed in one part recorded with the linear CCD array. In the longwave part of the spectrum, the number of neon lines decreased considerably, and the lines of other gases, for example, water vapor absorption lines were used along with the neon lines as reference ones. In the region of $10000\text{--}11000 \text{ cm}^{-1}$ these lines were repeatedly recorded with Fourier transform spectrometers, and their parameters are known quite well.⁶

The studies showed that the relative accuracy of measuring line positions by this method achieved 0.003 cm^{-1} .

7. *The threshold sensitivity of the spectrometer,* that is, the minimum detectable absorption coefficient, can be determined from the Bouguer law

$$I = I_0 \exp(-KL), \quad (4)$$

where L is the length of the absorbing layer; I_0 and I are the intensities of the incident radiation and the radiation transmitted through the absorbing layer; K is the absorption coefficient.

At low values of $K_{\text{thr}}L$ the exponent is expanded into a series and, restricting our consideration to the first term, we obtain

$$K_{\text{thr}} = \frac{1}{L} \frac{\Delta I}{I_0}, \quad \Delta I = I_0 - I. \quad (5)$$

The spectrometer sensitivity is restricted, in the first turn, by the instrument noise. The relation between different types of noise may be different, and usually one type is dominant and determines the threshold sensitivity. The first and strongest type of noise is the dark current, that is, the signal corresponding to no input radiation. The dark current signal includes a constant component, whose value is connected with peculiarities of the recording system, and a variable component caused by different dark current in every element. The dark current signal is recorded, stored, and then subtracted element-by-element from the signal in the following measurements. Simultaneously, ambient background illumination,

which may be observed in the absence of the signal, is subtracted.

Another type of noise is the noise of the source due to fluctuations in the intensity of the incident radiation. This noise significantly decreases at accumulation of the signal. Figures 4 and 5 exemplify the recorded spectra: dark current signal ($\sim 2\text{--}4\%$ of the signal), absorption spectrum of atmospheric air with and without noise, as well as in the case of signal accumulation ($N = 1, 100, \text{ and } 1000$). As a result, at accumulation of 1000 signals we obtained the signal-to-noise ratio in the IR region as high as 10^3 .

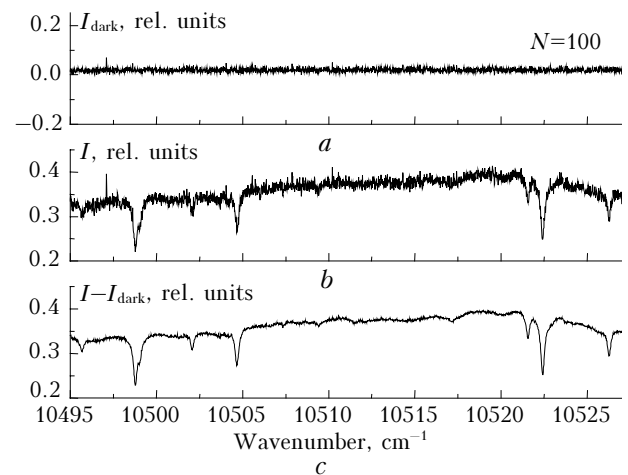


Fig. 4. Subtraction of the dark current signal: dark current signal (a); absorption spectrum of atmospheric air with the dark noise (b); absorption spectrum of atmospheric air without noise (c).

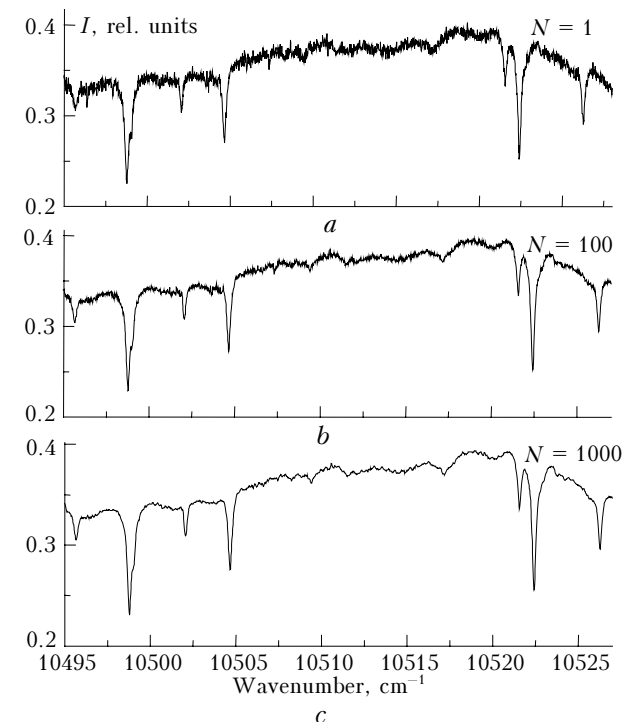


Fig. 5. Absorption spectrum of atmospheric air at accumulation of 1 (a), 100 (b), and 1000 signals (c).

Thus, the minimum measurable value of $\Delta I/I$ is 10^{-3} , which corresponds to the 10^{-5} cm^{-1} threshold value of the absorption coefficient recorded with the spectrometer in a 1-m long absorbing layer.

The parameters of the grating polychromator with the multichannel photodetector are given below.

Spectral region, cm^{-1}	10000–16000
Threshold sensitivity for the absorption coefficient at the cell length of 1 m, cm^{-1}	10^{-6} – 10^{-5}
Relative accuracy of the absorption coefficient measurements, %.....	3
Accuracy of line positions measurements, cm^{-1}	0.003
Spectral resolution, cm^{-1}	0.036
Signal-to-noise ratio (accumulation of 1000 signals) in the IR region.....	10^3
in the visible region.....	10^4

4. Measurement of the intensity ratio between the ortho- and para-components of the H_2O lines

The water vapor molecule exists in two isomers having different value of the nuclear spin: the so-called ortho- and para-modifications.⁷ The parallel orientation of the spins of hydrogen nuclei forms the ortho-isomer of the water molecule, while the antiparallel one forms the para-isomer. Ortho- and para-isomers exist as two different substances, their ratio under normal conditions is stable, and the statistical weight ratio of ortho- to para-water is equal to three. This effect manifests itself in the intensity ratios of pairs of spectral lines corresponding to these isomers. Since this ratio is fulfilled with very high accuracy, its measurement in a spectrum can serve as a criterion of the accuracy of spectrometric measurements of the absorption coefficients.

In the spectrum recorded we found several such pairs of spectral lines corresponding to different water isomers. Figure 6 shows water vapor lines centered at 10521.5677 and $10522.4227 \text{ cm}^{-1}$ recorded in atmospheric air at the total pressure of 1 atm.

The line profiles include up to 50 CCD elements, and they are well described by the Lorentz profile. The measured intensity ratio for the spectral lines corresponding to ortho- and para-water was 2.965, which confirms the 3% accuracy in relative measurements of line intensities.

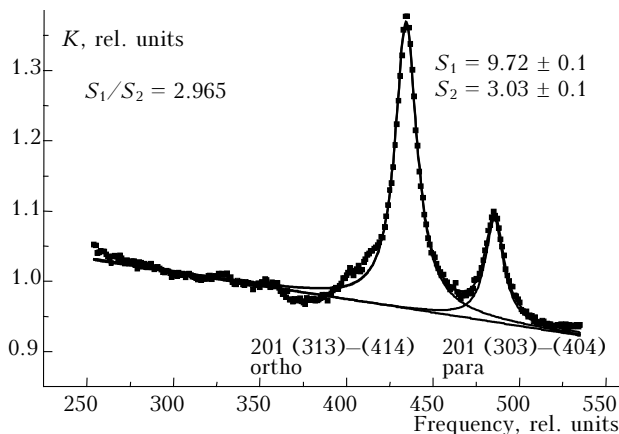


Fig. 6. Air pressure broadened H_2O absorption lines.

Acknowledgments

We are thankful to our colleagues Yu.A. Poplavskii and A.P. Shcherbakov for the great work in designing and fabrication of the recording system.

This work was accomplished within the framework of the "Optical Spectroscopy and Frequency Standards" Program of the Russian Academy of Sciences and partly supported by the Russian Foundation for Basic Research (Grants No. 02–03–32512 and No. 03–02–16471).

References

1. D.V. Dmitriev, Yu.A. Poplavskii, L.N. Sinita, Yu.A. Matul'yan, and A.P. Shcherbakov, *Atmos. Oceanic Opt.* **15**, No. 9, 704–707 (2002).
2. A.N. Zaidel, G.V. Ostrovskaya, and Yu.I. Ostrovskii, *Technology and Practice of Spectroscopy* (Nauka, Moscow, 1972), 375 pp.
3. V.I. Malyshev, *Introduction to Experimental Spectroscopy* (Nauka, Moscow, 1979), 478 pp.
4. V.V. Lebedeva, *Experimental Optics* (Moscow State University Press, Moscow, 1994), 364 pp.
5. A.P. Zaidel, V.K. Prokof'ev, and S.M. Raiskii, *Tables of Spectral Lines* (Gostekhizdat, Moscow, 1952), 560 pp.
6. J.-P. Chevillard, J.-Y. Mandin, and C. Camy-Peyret, *Can. J. Phys.* **67**, 1065–1084 (1988).
7. G. Herzberg, *Infrared and Raman Spectra of Polyatomic Molecules* (D. Van Nostrand, 1959).